HEAT TRANSFER ENHANCEMENT DUE TO CAVITIES IN IMPINGING JETS

Andrew J C King
Curtin University of Technology
Department of Mechanical Engineering
Fluid Dynamics Research Group
Perth, Australia
andrew.king@curtin.edu.au

Tilak T Chandratilleke
Curtin University of Technology
Department of Mechanical Engineering
Perth, Australia
Australia
t.chandratilleke@curtin.edu.au

ABSTRACT

This paper presents results from a study into the effectiveness of surface cavities in achieving increased heat transfer rates in impinging fluid jets. In this work a cylindrical cavity with an isothermally heated base was introduced beneath a steady fluid jet. The effects on the total heat transfer rate from the cavity were evaluated in a parametric study. Cavity depths up to 6 times the jet diameter were investigated at a range of Reynolds numbers and jet to surface distances. The key parameters affecting the heat transfer were found to be the Reynolds number and the distance between the jet nozzle exit and the cavity base. The effects of these parameters are discussed, and a useful range for each is identified with respect to heat transfer enhancement. The cavity arrangement was found to significantly enhance the heat transfer with the maximum heat transfer from the cavity found to be 33% higher than the heat transfer from a similarly heated flat plate.

NOMENCLATURE

z Jet to Surface Distance
h Cavity Depth
l Net Cavity Depth
d Jet diameter
z^* Dimensionless Jet to Surface Distance, z/d
h^* Dimensionless Cavity Depth, h/d
l^* Dimensionless Net Cavity Depth, l/d
d_c Cavity diameter
k_f Fluid conductivity
$\dot{q}$ Heat transfer rate through cavity base
ΔT Jet to cavity base temperature difference
$\overline{\text{Re}}$ Reynolds Number, $V_j d/\nu$
$\overline{\text{Nu}}$ Nusselt Number, $h_c d/k_f$

INTRODUCTION

With the continuous drive towards more efficient energy usage, and in combination with increasing miniaturisation of electronic devices, novel techniques for improving heat transfer processes are constantly sought. Impinging fluid jets are well known to provide amongst the highest heat transfer rates for single phase heat transfer [1]. As such, many schemes that seek to further increase heat transfer rates have been proposed and investigated. These schemes have included surface roughening, surface protrusions, concave and convex surfaces, and non-orthogonal impingement, amongst others [2–7]. Continuing along these lines, this paper presents and evaluates a novel scheme to increase heat transfer characterised by the introduction of a cavity beneath the jet orifice.

The simplest impinging jet system consists of a fluid jet discharging from a tube and impinging on a surface from which heat is to be removed or supplied. In this configuration, the fluid is forced through a 90° change in direction. This causes a stagnation region to develop beneath the jet, and a region of high heat transfer to form. In the present work, this system is modified by including a cavity in the target surface, directly beneath the stagnation point as shown in Figure 1. The primary effect of the cavity is to force the fluid to undergo a second 90° change in direction. As a consequence, a stagnation region is formed at the junction of the base and cavity wall, which in-turn acts to create a second region of high heat transfer in the system. With suitable selection of cavity dimensions and jet Reynolds number this paper demonstrates that a significantly higher overall heat transfer rate can be achieved from the system, compared with a 'conventional' fluid jet impinging normally on a heated flat plate.

PROBLEM FORMULATION

The system studied in the current work consisted of an axisymmetric jet discharging into a cylindrical cavity. The base of the cavity was isothermally heated, while the side of the cavity and all other surfaces were treated as adiabatic. A constant cavity diameter of twice the jet diameter was studied over a range of Reynolds numbers. In addition to varying the Reynolds number, the distance between the jet nozzle exit and the target
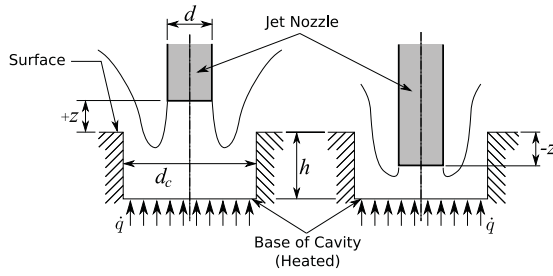
Figure 1.   FLUID JET IMPINGING INTO A HEATED CAVITY

Table 1.   PARAMETER RANGES

Parameter		Values
Cavity diameter	d_c/d	2
Jet to surface distance	z^*	-2, -1, 0, 1, 2
Cavity Depth	h^*	0, 1, 2, 3, 4
		5, 6, 7, 8
Reynolds Number	Re	5000, 10000
		20000, 30000

Figure 2.   TYPICAL COMPUTATIONAL MESH

surface was varied, as was the depth of the cavity. Figure 1 shows a schematic of the jet and cavity, indicating the critical dimensions. A key point to note in this figure is that both configurations where the jet nozzle discharged above the surface, and configurations where the jet nozzle protruded into the cavity were studied in this work.

Heat Transfer

In order to gauge how the cavity geometry affected the heat transfer, the average Nusselt number at the base of the cavity was calculated. For an isothermally heated cavity base such as considered in this work, this is calculated as

$$\overline{\mathrm{Nu}} = \frac{4\dot{q}d}{\pi d_c^2 k_f \Delta T} \tag{1}$$

Additionally, the local Nusselt number across the base was determined in a similar manner, from

$$\mathrm{Nu} = \frac{4q''d}{k_f \Delta T} \tag{2}$$

where q'' is the local heat transfer rate per unit area.

Parameter Ranges

The range of parameters investigated in this study are presented in Table 1. An additional parameter, the *net cavity depth*, was developed by combining the jet to surface distance, z, and the cavity depth, h, such that

$$l = z + h \tag{3}$$

This parameter is represents the distance between the jet nozzle and the cavity base, and was a key parameter characterising the observed heat transfer. The parameters selected for this study were non-dimensionalised with respect to the jet diameter. Values for cavity depth and jet to surface distance were chosen such that the range of net cavity depths studied was between 1 and 6.

Solution Technique

To solve for the flow and temperature field in the impinging jet-cavity system the Computational Fluid Dynamics software FLUENT was used. FLUENT uses a finite volume approa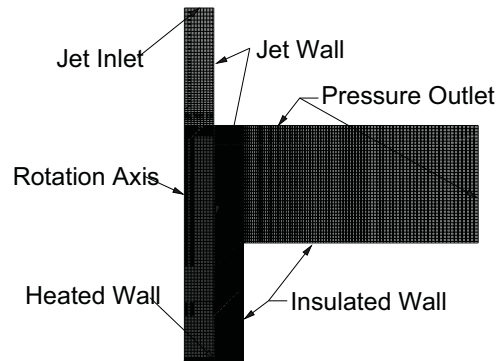ch to solving the Navier-Stokes equations, while an additional uncoupled transport equation is solved for the energy in the system. The $\overline{v}^2$-f turbulence model also requires three additional transport equations to be solved for, k, ε and $\overline{v}^2$, in addition to an elliptic equation for f.

Solution Domain

The solution domain for the simulated case is shown in Figure 2. Due to the change in geometry as the cavity depth was varied, it was necessary to construct a new computational mesh for each cavity depth investigated. A typical mesh is shown in Figure 2.

Boundary Conditions

Fluid   For fluid modelling, the boundary conditions were selected as follows. At the inlet a fully developed flow profile was applied, where the velocity and turbulence parameters were taken from a separate model of fully-developed pipe flow. For the outlet boundaries at the top and side of the domain, a constant static pressure was applied. Inflow was allowed at these boundaries, and where it occurred the velocity was calculated based on the pressure differential between the internal domain and specified outlet value. All solid walls of the domain were treated as non-slip.

Thermal   For thermal modelling, the following boundary conditions were applied. At the inlet, a constant inlet temperature of 300 K was set for the incoming fluid. The base of the cavity was treated as an isothermal surface, with a temperature
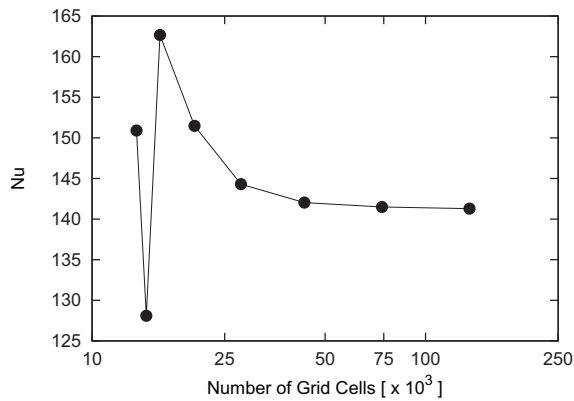
Figure 4. VARIATION IN AVERAGE NUSSELT NUMBER AT THE CAVITY BASE Re=20,000, z^*=0, h^*=2.

Figure 5. LOCAL NUSSELT NUMBER FOR A FLAT PLATE AT A REYNOLDS NUMBER OF 23,000. BS89 – [12], BH91 – [13], CJ93 – [14]

of 325 K, 25 K above the jet inlet temperature. The sides of the cavity were treated as adiabatic, to allow the influence of the cavity to be studied in isolation, as were the remaining solid surfaces. For the outlet boundaries, a zero-normal-gradient on temperature was applied to fluid exiting the domain, while where inflow occurred a prescribed temperature, equal to the jet inlet temperature, was applied.

Turbulence Modelling

Typically for general engineering type flow, a variant of the k-ε turbulence model is used to account for turbulence in the system. For impinging jet flows, however, these models fail to capture turbulence accurately, which in turn leads to extremely poor prediction of heat transfer and energy transport [8, 9]. For these flows a low-Reynolds number turbulence model is necessary for accurate heat transfer predictions. The $\bar{v}^2$-f model [10] has been shown to give good agreement with experimental results [9, 11].

VALIDATION
Grid Independence

For each of the meshes used for simulation, a grid independence study was performed at the highest flowrate. In addition the refinement near the solid surfaces was checked to ensure that the y^+ values were below 1, a requirement of the $\bar{v}^2$-f turbulence model used in the work. Figure 4 shows the results of the grid independence study for one grid, at a jet to surface distance of $z^* = 0$ and $h^* = 2$.

Code Validation

Due to the novel nature of the proposed cavity scheme no existing experimental work to validate the model could was found in the literature. This work is currently being undertaken, however until these results are available, validation of the numerical code is made by comparison with experimental data for the reference flat plate case only. Figure 5 shows a comparison of the local Nusselt number for a jet to surface distance of $z^* = 2$, at a Reynolds number of 23,000.
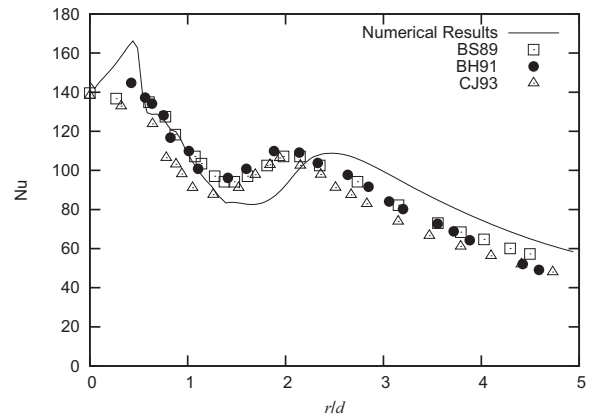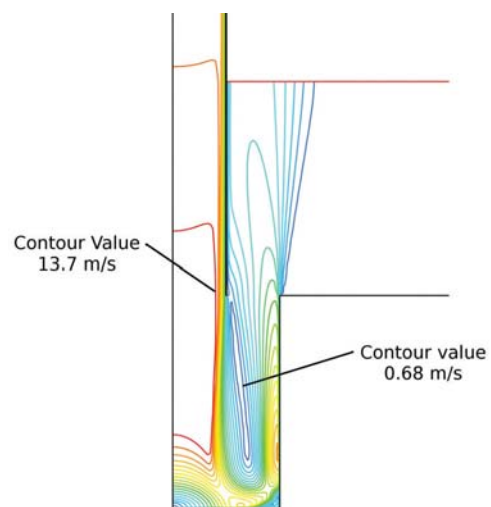

Figure 6. CONTOURS OF VELOCITY MAGNITUDE FOR $z^* = 0$, $h^* = 2$, Re = 20,000

RESULTS & DISCUSSION
Flow Field

Figure 6 shows the velocity vectors for a jet to surface distance of $z^* = 0$, a cavity depth of $h^* = 2$ and at a Reynolds number of 20,000. This figure indicates a typical flow field for the jet and cavity arrangement. Two stagnation regions are clearly visible at the heated surface, one occurring at the centre of the cavity base and one occurring at the cavity edge.

Average Nusselt Number

Figure 3 shows the average heat transfer rate, indicated by the average Nusselt number at the base of the cavity, over the range of parameters studied. Examining these figures, it is clear that the key parameters affecting the observed heat transfer are the jet Reynolds number, and the net cavity depth. To a lesser extent, the observed change in heat transfer was also found to be dependent on the actual cavity depth, and on the jet to surface distance.

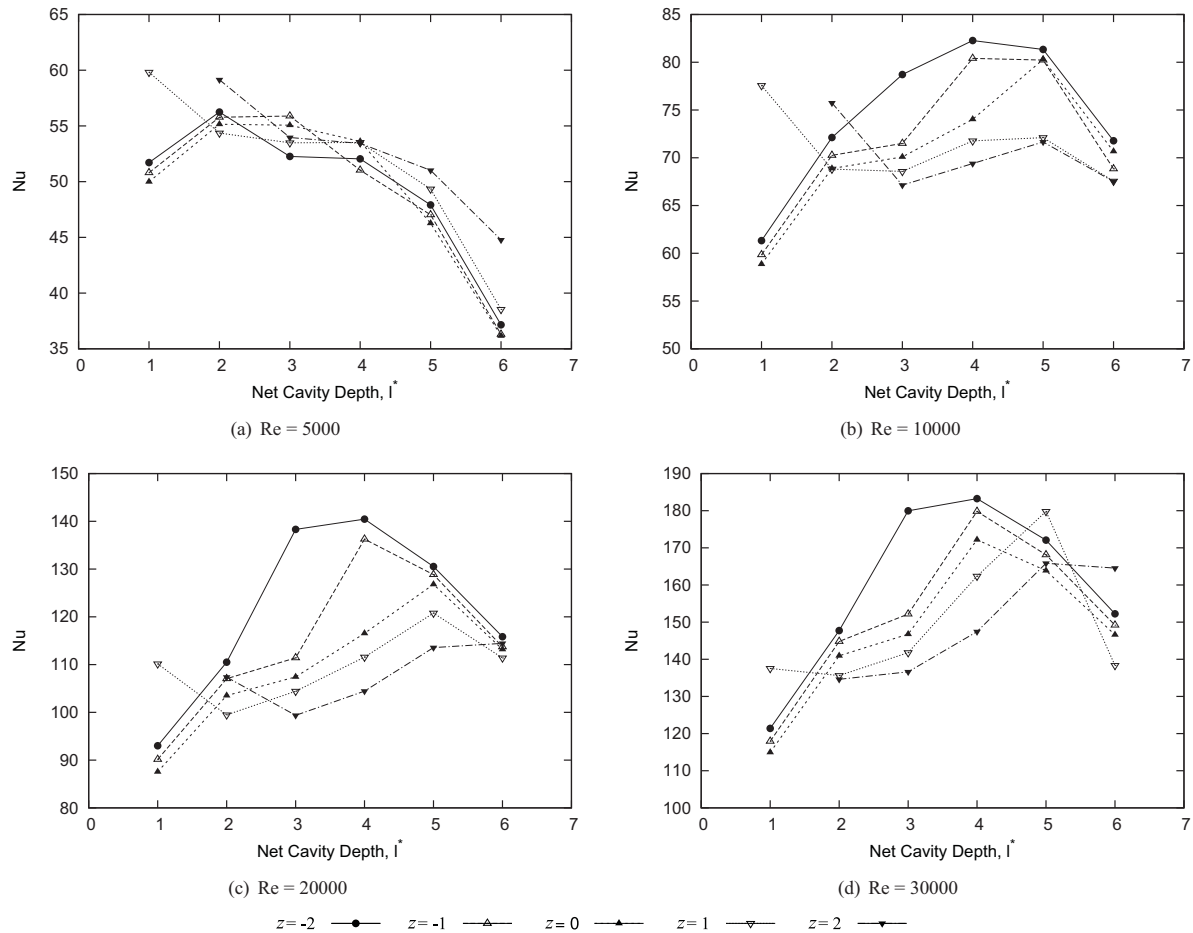Starting with Figure 3(a), at this flow speed the introduction

(a) Re = 5000

(b) Re = 10000

(c) Re = 20000

(d) Re = 30000

$z = -2$ ——●—— $z = -1$ ——△—— $z = 0$ ——▲—— $z = 1$ ——▽—— $z = 2$ ——▼——

Figure 3.   AVERAGE NUSSELT NUMBER OVER CAVITY BASE

of the cavity to the flat plate tended to decrease the heat transfer observed from the base of the cavity. For the cases where the jet nozzle discharged above the reference surface, this drop in heat transfer was larger when the cavity was initially introduced into the flat plate, for $z^* = 1$ with l^* changing from 1 to 2, and at $z^* = 2$ with l^* changing from 2 to 3. For the cases where the jet nozzle was level with or below the reference surface, the heat transfer increased as the net cavity depth increased from 1 to 2, but decreased as the cavity depth was further increased.

Conversely, Figure 3(d) shows that at a Reynolds number of 30,000 heat transfer improvement is possible in all of the investigated cases. Initially, for the two cases where the jet discharged above the surface, introducing the cavity beneath the jet initially had minimal change on the observed heat transfer. However as the cavity depth was increased further, the observed heat transfer increased significantly, until the net cavity depth reached 5, after which the heat transfer started to decrease. For the cases where the jet discharged level with or below the height of the reference surface, the heat transfer increased sharply until a net cavity depth of 4 was reached, after which the heat transfer again started to decrease.

At intermediate Reynolds numbers, behaviour between these two extremes was observed. At a Reynolds number of 10,000 and for cases where the jet nozzle was above the surface, the heat transfer was always highest where there was no

cavity present, for $z^* = 1$ and $l^* = 1$ and for $z^* = 2$ and $l^* = 2$. For the cases where the jet discharged level with or below the reference surface, the heat transfer increased as the cavity depth was increased, until the net cavity depth was equal to 4.

At a Reynolds number of 20,000 for the cases where the jet nozzle was above the surface, the heat transfer initially decreased. As the depth of the cavity was increased further, however, the heat transfer was observed to increase up until the net cavity depth was equal to 5. For the cases where the cavity was level with the surface, the heat transfer was always observed to increase, until the net cavity depth was equal to 4.

Local Nusselt Number

Figure 7 shows the local Nusselt number across the base of the cavity for a jet protruding two jet diameters into the cavity, at Reynolds numbers of 5000 and 30,000. Figure 8 shows the local Nusselt number across the base of the cavity for a jet discharging two jet diameters above the reference surface, at at Reynolds numbers of 5000 and 30,000.

In both figures and at a Reynolds number of 5000, the heat transfer across the base of the cavity was relatively uniform, though the effect of the second stagnation point can be seen near the sides of the cavity, where $r/d = 1$. For the case where the jet discharges above the reference surface ($z^* = 2$), the heat transfer near the sides of the cavity decreased as the cavity depth
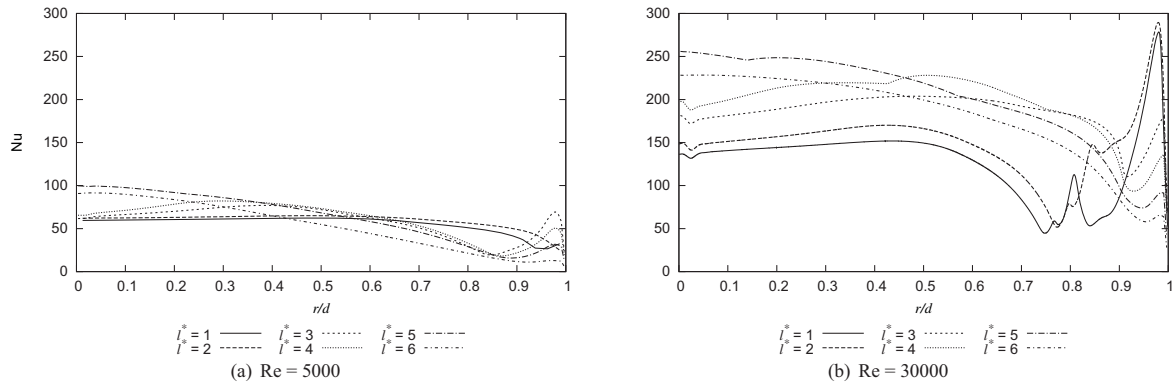
(a) Re = 5000

(b) Re = 30000

Figure 7.   LOCAL NUSSELT NUMBER ACROSS BASE OF CAVITY FOR $z^* = -2$, CENTRE AT $r = 0$
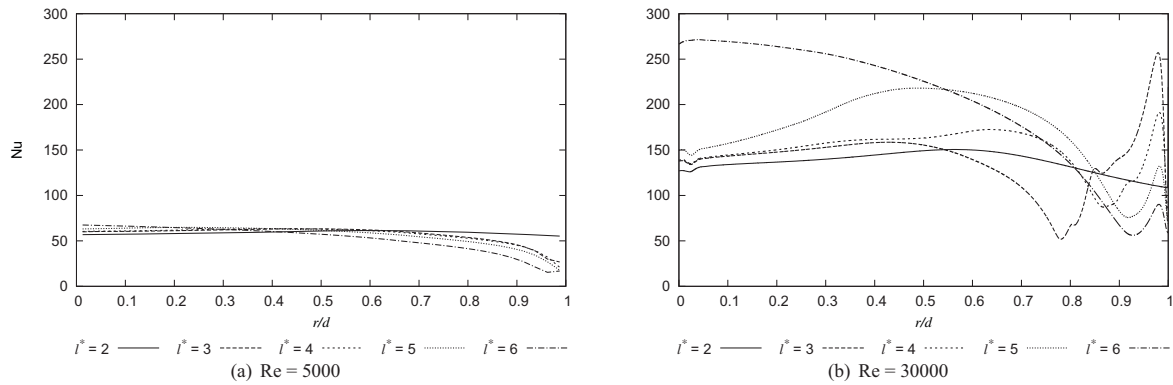

(a) Re = 5000

(b) Re = 30000

Figure 8.   LOCAL NUSSELT NUMBER ACROSS BASE OF CAVITY FOR $z^* = 2$, CENTRE AT $r = 0$

was increased, whereas at the centre ($r/d = 0$), there was little change in the local Nusselt number. When the jet protruded into the cavity ($z^* = -2$), the heat transfer was again observed to decrease near the sides of the cavity. In this case, the heat transfer near the centre increased, though this increase was not large enough to offset the decrease in heat transfer near the side.

At a Reynolds number of 30,000, the effect of the cavity depth was more pronounced, for both jet to surface distances. In the cases where the jet discharged above the surface, the heat transfer at the centre is similar in most cases, apart from at a net cavity depth of 6, where the heat transfer was much higher. Moving towards the side of the cavity, the heat transfer first reduced (at $r/d \sim 0.8 - 0.9$) followed by an increase closer to the side of the cavity ($r/d \sim 0.95$).

A similar drop-off in heat transfer in the region near $r/d \sim 0.8 - 0.9$, followed by an increase at $r/d \sim 0.95$, was evident for the case where the jet protruded into the cavity. In this case, however, the heat transfer at the centre varied significantly as the cavity depth increased. The minimum observed heat transfer at the cavity centre was observed at the lowest net cavity depth, while the heat transfer increased as the cavity depth increased. The maximum heat transfer at the centre was reached at a net cavity depth of 5, after which the heat transfer again reduced.

It should be noted that at a Reynolds number of 30,000 the variation in local Nusselt number across is reasonably high. Depending on the particular application of this cooling technique, this could cause large thermal gradients to be created. Whether these gradients would result in unacceptable thermal stresses would need to be examined on a case by case basis.

Heat Transfer Enhancement

From the previous sections it is clear that in many cases heat transfer enhancement can be achieved by introducing a cavity beneath an impinging jet. In particular, Figure 3 shows that for Reynolds numbers above 5000, heat transfer enhancement is possible in every case, as long as the correct configuration of the jet and cavity is selected.

To quantify the possible heat transfer enhancement, it was necessary to identify a reference level of heat transfer for comparison. In the parametric study, two geometries represent a conventional fluid jet impinging on a flat plate. These geometries were those where $z^* = 2$, and $h^* = 0$ ($l^* = 2$), and where $z^* = 1$ and $h^* = 0$ ($l^* = 1$).

For each Reynolds number, the reference heat transfer rate was taken to be the higher of the heat transfer rates for each of these cases and the maximum heat transfer was compared to this value.

The maximum improvement in heat transfer was observed with the same configuration at all Reynolds numbers, namely for a net cavity depth of 4 (l^*), and with the jet protruding 2 jet diameters into the cavity ($z^* = -2$). The magnitudes of the relative increases were 6.07 %, 27.50 % and 33.10 % for Reynolds numbers of 10,000, 20,000 and 30,000 respectively.

CONCLUSIONS

This paper examined the effects on the heat transfer rate due to the introduction of a cylindrical, axially aligned cavity beneath a normally impinging jet. A single cavity diameter, equal to twice the jet diameter, was studied over a range of cavity depths, jet heights and Reynolds numbers.

The results from the parametric study show that in general there is significant potential for increasing the heat transfer with a suitable cavity and jet geometry. The results indicate a high dependence on the Reynolds number, with a Reynolds number of 5000 showing no increase in heat transfer. For Reynolds numbers above and equal to 10,000 it was possible to increase the heat transfer rates in all cases. The maximum increase was observed with a dimensionless net cavity depth equal to 4, compromising of a total (dimensionless) cavity depth of 6, with the jet protruding 2 jet diameters into the cavity. The magnitudes of the increases were 6.1, 27.5 and 33.1 % compared to an equivalent flat plate case, for Reynolds numbers of 10,000, 20,000 and 30,000 respectively. For cases where heat transfer takes place from the side of the cavity, it is expected that even higher increases in heat transfer should be possible.

REFERENCES

[1] Mudawar, I., 2001. "Assessment of high-heat-flux thermal management schemes". *IEEE Transactions on Components and Packaging Technologies,* **24**(2), pp. 122–141.

[2] Mesbah, M., Baughn, J. W., and Yap, C. R., 1996. "The effect of curvature on the local heat transfer to an impinging jet on a hemispherically concave surface". In The ninth international symposium on transport phenomena in thermal-fluids engineering, pp. 795–800.

[3] Beitelmal, A. H., Saad, M. A., and Patel, C. D., 2000. "Effects of surface roughness on the average heat transfer of an impinging air jet". *International Communications in Heat and Mass Transfer,* **27**, pp. 1–12.

[4] Beitelmal, A. H., Saad, M. A., and Patel, C. D., 2000. "The effect of inclination on the heat transfer between a flat surface and an impinging two-dimensional air jet". *International Journal of Heat and Fluid Flow,* **21**, pp. 156–163.

[5] Lee, D. H., Chung, Y. S., and Kim, M. G., 1999. "Turbulent heat transfer from a convex hemispherical surface to a round impinging jet". *International Journal of Heat and Mass Transfer,* **42**, pp. 1147–1156.

[6] King, A. J. C., and Chandratilleke, T. T., 2004. "Turbulence modelling of impinging jets for high heat flux cooling applications". In International Conference on Computational Methods, G. R. Liu, V. B. C. Tan, and X. Han, eds., pp. 177–182.

[7] Chang, S. W., and Liou, H.-F., 2009. "Heat transfer of impinging jet-array onto concave- and convex-dimpled surfaces with effusion". *International Journal of Heat and Mass Transfer,* **52**, pp. 4484–4499.

[8] Craft, T. J., Graham, L. J. W., and Launder, B. E., 1993. "Impinging jet studies for turbulence model assessment – II An examination of four turbulence models". *International Journal of Heat and Mass Transfer,* **36**, pp. 2685 – 2697.

[9] King, A. J. C., and Chandratilleke, T. T., 2004. "Heat transfer enhancement in impinging jets by surface modifi-

cation". In 6th Electronics Packaging Technology Conference, pp. 270–272.

[10] Durbin, P. A., 1991. "Near wall turbulence closure without damping functions.". *Theoretical and Computational Fluid Dynamics,* **3**, pp. 1–13.

[11] Behnia, M., Parneix, S., Shabany, Y., and Durbin, P. A., 1999. "Numerical study of turbulent heat transfer in confined and unconfined impinging jets". *International Journal of Heat and Fluid Flow,* **20**, pp. 1–9.

[12] Baughn, J. W. B., and Shimizu, S., 1989. "Heat transfer measurements from a surface with uniform heat flux and an impinging jet". *ASME Journal of Heat Transfer,* **111**, p. 1096.

[13] Baughn, J. W., Hechanova, A. E., and Yan, X., 1991. "An experimental study of entrainment effects on the heat transfer from a flat surface to a heated circular impinging jet". *Transactions of the ASME Journal of Heat Transfer,* **113**, pp. 1023–1025.

[14] Cooper, D., Jackson, C., Launder, B. E., and Liao, G. X., 1993. "Impinging jet studies for turbulence model assessment – I Flow-field experiments". *International Journal of Heat and Mass Transfer,* **36**, pp. 2675 – 2684.